Neurite Imaging

DOI: 10.1002/anie.200702617

Neurite Imaging of Living PC12 Cells with Scanning Electrochemical/Near-Field Optical/Atomic Force Microscopy**

Akio Ueda, Osamu Niwa, Kenichi Maruyama, Yutaka Shindo, Kotaro Oka, and Koji Suzuki**

The mechanisms of intercellular communication are important with respect to neurite formation and signal transmission between nerve cells. Scanning electrochemical microscopy (SECM) has played a prominent role in fields of neuroscience such as single-cell surface reactions.[1,2] As the result of further investigations of biological systems, hybrid SECM systems integrated with surface plasmon resonance (SPR),[3] atomic force microscopy (AFM), and fluorescent spectroscopy (FS)[4] have been developed to provide information on physical structures and chemical reactions simultaneously. Shear-force-based SECM/AFM techniques have definite advantages as they allow the topographical and electrochemical imaging of individual cells,[5] diffusion from a nanopore,[6] and enzyme activity.[7] In contrast, optical methods are capable of imaging inner cell reactions and have been combined with SECM. Bard and co-workers reported shear-force-based SECM/optical microscopy (OM).[8] We have also reported a nanometer-sized straight optical fiber electrode for SECM/OM,[9] and employed it to obtain topographical images of PC12 neurites. More recently, Matsue and co-workers reported a combined SECM/near-field optical microscopy (NSOM)/AFM technique capable of three-mode imaging in standing-approach mode.[10]

However, the topographical and electrochemical resolution for such hybrid SECM techniques is commonly on the order of micrometers because it is governed by the tip size of the probe and the distance between tip and sample. For accurate distance control, Kranz and co-workers reported a dynamic force mode AFM system with an integrated submicrometer-sized electrode that has an insulated apex.[7] This system can realize submicrometer resolution, whereas the conventional shear-force system can achieve only micrometer resolution. However, for cell surface imaging and the detection of neurotransmitters such as the zeptomolar concentrations of released catecholamine,[11] the insulated apex must be shorter so that the electrode can be brought as close as possible to the sample without touching it.

Herein, we demonstrate improved resolution imaging by using a hybrid SECM/NSOM/AFM technique in the dynamic-force mode with a protection layer system to prevent direct contact between the electrode and sample. When insulating polymer (Figure 1a) fabricated with a focused ion beam (FIB) at an angle of 60 degrees to the tip axis is used as a protective layer (Figure 1b), the electrode part can be located on the nearer edge so that the electrode area and the distance between the tip and the sample can be decreased. The edge of the ring electrode nearer to the imaging target mainly contributes to the SECM detection because decreasing the distance between the probe and the sample increases the variation in the SECM signal. In Figure 1c, the protective layer theoretically keeps the distance between the electrode and the sample at only 100 nm. By applying this technique in proximity to the cell, we can simultaneously obtain chemical information from near the outer membrane and optical information about the membrane and cytoplasm by using SECM and NSOM, respectively, at the submicrometer level, whereas the images obtained with previously reported hybrid SECM techniques are typically limited to cell bodies because of their resolution. We applied this three-mode imaging to the neurites of Fluo-4-labeled PC12 cells.

The tip was fabricated according to our previous report.[9] To obtain submicrometer resolution, a novel bent probe (Figure 2a) was employed for the dynamic force mode system, and the tip was fabricated with the FIB process. The tip had an approximately 100-nm aperture surrounded by a 250-nm gold-ring electrode, and an outermost electrophoretic insulating polymer, which we confirmed with a scanning electron microscopy (SEM) image (Figure 2b). When this bent probe approaches the sample at a certain angle, the outermost insulating polymer functions as a protective layer. The voltammetric responses from the electrode with 10 mM

[*] A. Ueda, Prof. O. Niwa
National Institute of Advanced Industrial Science and Technology (AIST)
Central 6, 1-1-1 Higashi Tsukuba 305-8566 (Japan)
Fax: (+81) 29-861-6177
E-mail: niwa.o@aist.go.jp
A. Ueda, Prof. O. Niwa
Department of Electronic Chemistry
Interdisciplinary Graduate School of Science and Engineering
Tokyo Institute of Technology
4259 Nagatsuta-cho, Midori-ku, Yokohama 226-8503 (Japan)
Dr. K. Maruyama, Prof. K. Suzuki
Department of Applied Chemistry
Faculty of Science and Technology
Keio University
3-14-1 Hiyoshi, Kohoku-ku, Yokohama 223-8522 (Japan)
Fax: (+81) 45-566-1568
E-mail: suzuki@applc.keio.ac.jp
Y. Shindo, Prof. K. Oka
Department of Biosciences and Informatics
Faculty of Science and Technology
Keio University
3-14-1 Hiyoshi, Kohoku-ku, Yokohama 223-8522 (Japan)

[**] We thank M. Iyoki (SII Nano Technology Inc.) and Prof. T. Saiki (Keio University) for valuable conversations. This work was supported by JSPS Research Fellowship for Young Scientists and the Core Research for Evolutional Science and Technology (CREST) program of the Japan Science and Technology Agency (JST).

Supporting information for this article is available on the WWW under http://www.angewandte.org or from the author.

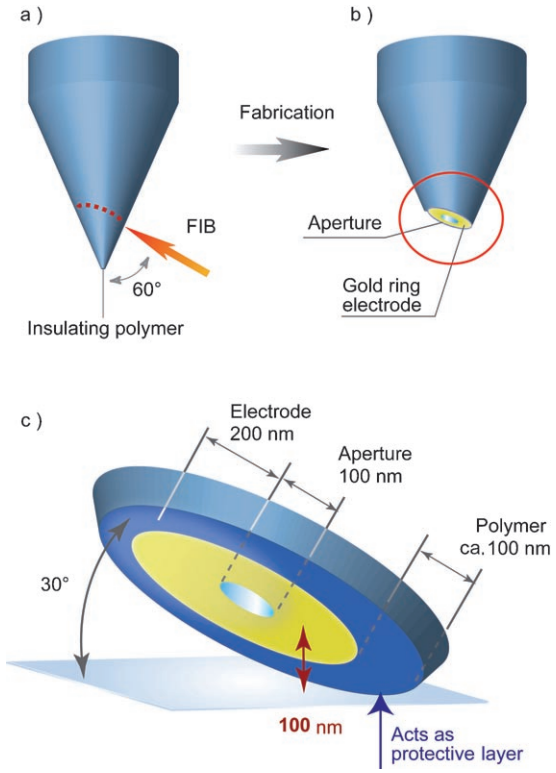

Figure 1. Conceptual diagram of the tip fabrication and dynamic force mode AFM system: The tip shape before (a) and after (b) the FIB process; c) enlargement of the circled area in (b) indicating the proximity of the tip to the sample in dynamic-force mode. The conductive electrode and sample are separated by a small gap filled with insulating polymer.

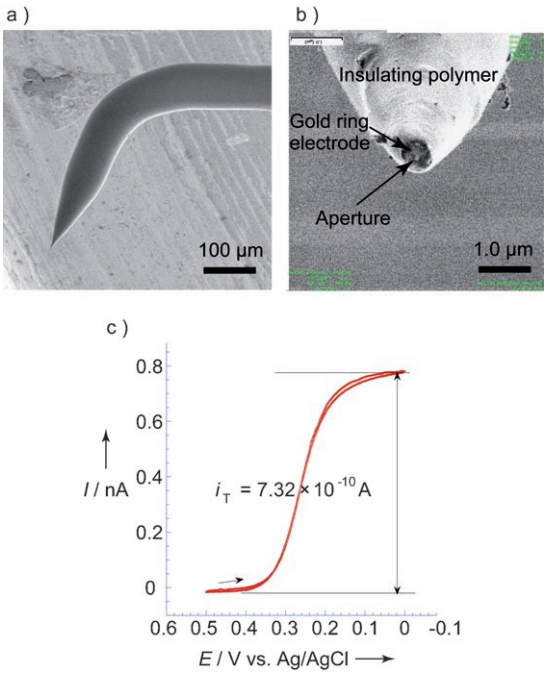

Figure 2. Topographical image and electrochemical properties of the probe: a) SEM image of a bent probe; b) FIB image of a tip with an aperture of 100 nm and a ring electrode radius of 300 nm; c) cyclic voltammogram of a tip in 10 mM $[Fe(CN)_6]^{3-}$ and 0.5 M KCl at a scan rate of 50 mV s^{-1}.

$[Fe(CN)_6]^{3-}$ in the presence of a supporting electrolyte (0.5 M KCl) showed sigmoidal curves and a diffusion-limited current of 7.32×10^{-10} A (Figure 2c). Although the tip appears to be a ring electrode, it is considered to be a disk electrode because the ratio of the radius of the gold part to that of the aperture is less than 1.25.[12] The radius of the electrode tip calculated as a disk electrode was 292 nm, which agreed well with the radius obtained from the SEM image (Figure 2b).

The performance obtained with the SECM/NSOM/AFM technique was confirmed by the acquisition of topographical and electrochemical images of gold dots (400-nm gold dots spaced with 1.0-µm glass and with a gold height of 50 nm) and topographical and near-field optical images of 100-nm fluorescent spheres (the preparation of these samples is described in the Supporting Information). The images of the 400-nm dots obtained with a bent probe ($r_{eff} = 136$ nm) in AFM mode (Figure 3a-1) corresponded to those obtained in

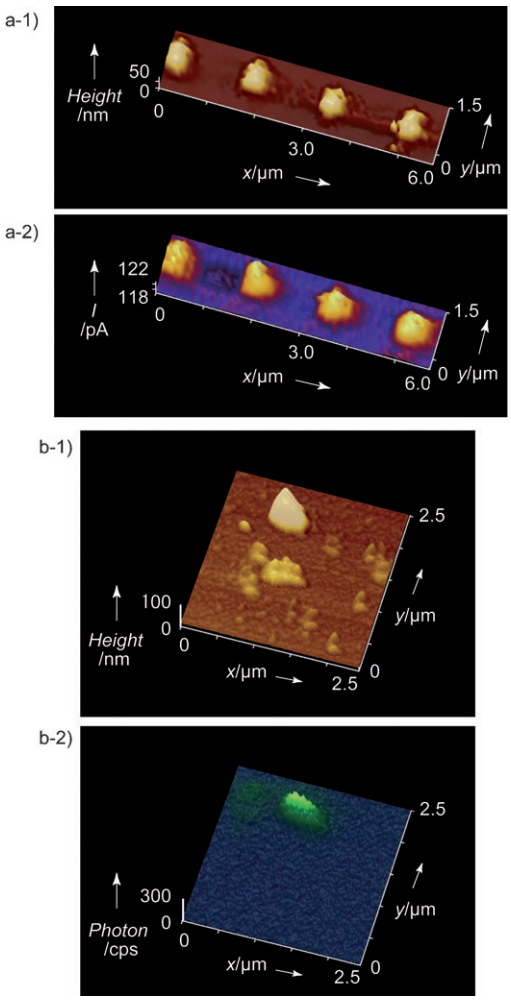

Figure 3. Topographical (a-1) and electrochemical (a-2) images of 400-nm gold dots with SECM/AFM, and topographical (b-1) and fluorescent (b-2) images of 100-nm fluorescent spheres with NSOM/AFM recorded by using a bent probe. Scan rate: 0.3 Hz. Electrochemical imaging (a-2) was performed at a probe potential of 0.5 V (vs. Ag/AgCl) in 3.0 mM ferrocenyl methanol and 0.5 M KCl. The fluorescence of the spheres (b-2) with a maximum emission wavelength of 520 nm excited at a wavelength of 488 nm by near-field optics from the tip was led to a avalanche photodiode detector through a band-pass filter.

SECM mode (Figure 3a-2). Although we obtained a relatively clear image of the submicrometer-order target, the image contrast is not high because the tip surface is tilted from the plane parallel to the substrate surface for dynamic force mode imaging. The approach curves in relation to the contrast are shown in the Supporting Information. In addition, the effect of positive feedback becomes weaker and the current approaches that for an infinite insulating substrate[13,14] when the tip size is similar to or larger than the unbiased conductive substrate. For imaging 400-nm dots, the tip size is not sufficiently small relative to the dot size and this may also reduce the contrast because of the low positive feedback effect. However, we obtained relatively clear images of 400-nm conductive areas in SECM mode by achieving accurate distance control with a protective layer and a submicrometer electrode. The resolution of each mode, which was measured with reference to a report by Lee et al.,[8] was 240 nm in AFM mode and 380 nm in SECM mode. Images of 100-nm fluorescent spheres obtained in AFM and NSOM modes are shown in Figure 3b-1 and 3b-2, respectively. The ellipsoid NSOM image reflects the ellipsoid aperture of the tip. The full width at half-maximum photon intensity of a 100-nm fluorescent sphere was 390 nm in the major axis and 180 nm in the minor axis, which is below the diffraction limit. These images indicate that all three modes have the potential to reveal the submicrometer structure or characteristic chemical sites on the neurites.

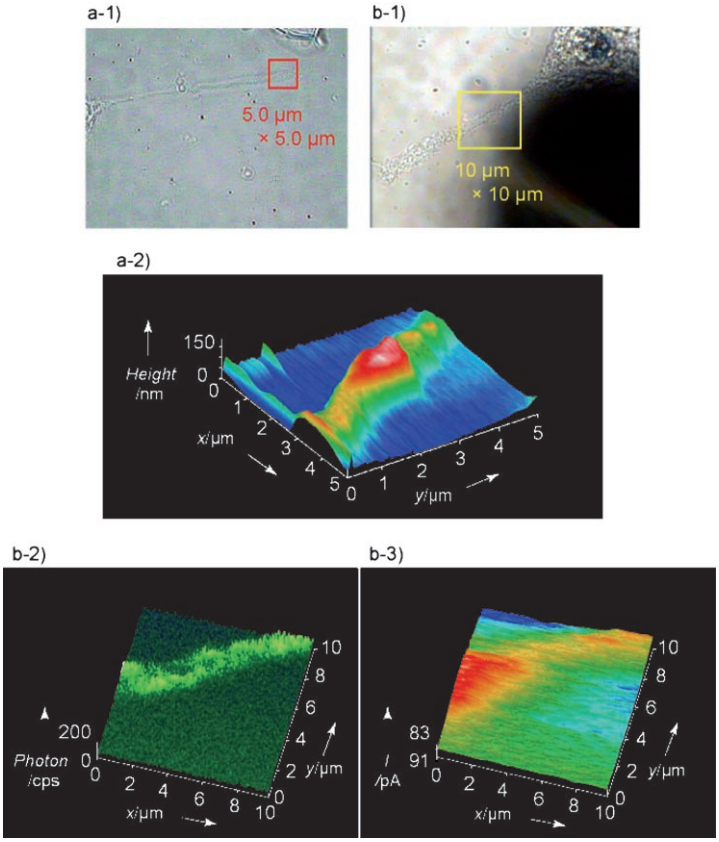

Figure 4. Optical images of control PC12 cells (a-1) and Fluo-4-labeled PC12 cells (b-1). The topographical image (a-2) was obtained by using the dynamic-force mode. Simultaneous near-field optical (b-2) and electrochemical (b-3) images were obtained in constant-height mode. Fluo-4 was excited from the near-field optics ($\lambda = 488$ nm) at the tip, and the emitted light was led to an avalanche photodiode through a band-pass filter. The tip ($r_{eff} = 105$ nm) was held at a potential of 0.5 V (vs. Ag/AgCl) in 50 mM HEPES buffer containing 3.0 mM ferrocenyl methanol. The working distance was set at less than 2.5 μm above the glass sample (see the Supporting Information). Scan rate: 0.3 Hz.

PC12 cells are well known as model neuronal cells, and the differentiation into neuron phenotypes is triggered by nerve growth factor (NGF).[15] Although SECM imaging of PC12 cells has been reported for various imaging modes including constant-height mode,[16] constant-current mode,[17] and shear force feedback mode,[10] detailed imaging has been limited to the PC12 cell body owing to its micrometer-order resolution. In contrast, neurites are attractive objects of study. For example, varicosity, which is related to the release of Ca^{2+} and neurotransmitters, only exists at neurites, which are very important for intercellular communication. However, it is difficult to image neurites and varicosities with a conventional SECM system, because neurites are smaller than a micrometer. Our SECM/NSOM/AFM technique allows us to image the topography and chemical reactions of the neurites of PC12 cells.

The tip was used for the topographical imaging of differentiated PC12 cell neurites within the red square in Figure 4a-1 by using the AFM mode. An AFM image is clearly obtained, as shown in Figure 4a-2. The submicrometer tip size and dynamic force mode system enable the measurement of the high-resolution topographical image. The PC12 cell neurites were 800 nm wide and 150 nm high, and their central swelling appeared to be varicosities whose size was previously determined from an SEM image.[18] As the AFM mode can cause a physical interaction, we evaluated the size of the PC12 neurites with both the AFM mode and SECM/NSOM in constant-height mode. For this purpose, the PC12 cells are labeled with a Ca^{2+} fluorescent marker, because Ca^{2+} plays an important role in neurotransmitter release[19] and apoptosis induction.[20] SECM/NSOM imaging was used for differentiated PC12 cell neurites (Figure 4b-1) within the yellow square. The images obtained in the NSOM mode (Figure 4b-2) correspond to the fluorescent labeled Ca^{2+} in the cell, and the SECM negative feedback mode (Figure 4b-3) corresponds to hindering of the diffusion of redox species toward the tip. This top right part of the inner cell Ca^{2+}-derived NSOM image corresponds well to the topographically derived SECM image, indicating that the Ca^{2+} distribution is the same size as the neurite width. In contrast, the width of the bottom left part obtained from the SECM image is more than that obtained from the NSOM image. This may be because the image reflects the inhomogeneous Ca^{2+} distribution in the neurites. These results show that our system enabled us to image both the distribution of the fluorescence strength near the inner membrane in the neurites and the subtle height differences between neurites simultaneously in the NSOM and SECM modes. We demonstrate the imaging of characteristic sites, such as varicosity-like structures and the distribu-

tion of Ca^{2+}, located at neurites in PC12 cells for the first time with our newly developed SECM/NSOM/AFM system.

Our system is capable of imaging submicrometer-order structures and characteristic chemical sites in three different modes with low submicrometer resolution in the dynamic-force mode with a thin protection layer. This system can be used for directly studying the dynamic activity of local cellular areas such as the relationship between inner cell Ca^{2+} level and dopamine release near a varicosity on a neurite.

Received: June 15, 2007
Revised: September 1, 2007
Published online: September 26, 2007

Keywords: neurites · PC12 cells · scanning electrochemical microscopy · scanning probe microscopy · surface analysis

[1] A. J. Bard, X. Li, W. Zhan, *Biosens. Bioelectron.* **2006**, *22*, 461.
[2] W. Feng, S. A. Rotenberg, M. V. Mirkin, *Anal. Chem.* **2003**, *75*, 4148.
[3] J. Xiang, J. Guo, F. M. Zhou, *Anal. Chem.* **2006**, *78*, 1418.
[4] F. M. Boldt, J. Heinze, M. Diez, J. Petersen, M. Borsch, *Anal. Chem.* **2004**, *76*, 3473.
[5] A. Hengstenberg, A. Blochl, I. D. Dietzel, W. Schuhmann, *Angew. Chem.* **2001**, *113*, 942; *Angew. Chem. Int. Ed.* **2001**, *40*, 905.
[6] J. V. Macpherson, C. E. Jones, A. L. Barker, P. R. Unwin, *Anal. Chem.* **2002**, *74*, 1841.
[7] A. Kueng, C. Kranz, A. Lugstein, E. Bertagnolli, B. Mizaikoff, *Angew. Chem.* **2003**, *115*, 3358; *Angew. Chem. Int. Ed.* **2003**, *42*, 3238.
[8] Y. Lee, Z. F. Ding, A. J. Bard, *Anal. Chem.* **2002**, *74*, 3634.
[9] K. Maruyama, H. Ohkawa, S. Ogawa, A. Ueda, O. Niwa, K. Suzuki, *Anal. Chem.* **2006**, *78*, 1904.
[10] Y. Takahashi, Y. Hirano, T. Yasukawa, H. Shiku, H. Yamada, T. Matsue, *Langmuir* **2006**, *22*, 10299.
[11] K. D. Kozminski, D. A. Gutman, V. Davila, D. Sulzer, A. G. Ewing, *Anal. Chem.* **1998**, *70*, 3123.
[12] Y. Lee, S. Amemiya, A. J. Bard, *Anal. Chem.* **2001**, *73*, 2261.
[13] C. G. Zoski, N. Simjee, O. Guenat, M. Koudelka-Hep, *Anal. Chem.* **2004**, *76*, 62.
[14] H. Xiong, J. D. Guo, S. Amemiya, *Anal. Chem.* **2007**, *79*, 2735.
[15] L. A. Greene, A. S. Tischler, *Proc. Natl. Acad. Sci. USA* **1976**, *73*, 2424.
[16] J. M. Liebetrau, H. M. Miller, J. E. Baur, S. A. Takacs, V. Anupunpisit, P. A. Garris, D. O. Wipf, *Anal. Chem.* **2003**, *75*, 563.
[17] R. T. Kurulugama, D. O. Wipf, S. A. Takacs, S. Pongmayteegul, P. A. Garris, J. E. Baur, *Anal. Chem.* **2005**, *77*, 1111.
[18] J. R. Jacobs, J. K. Stevens, *J. Cell Biol.* **1986**, *103*, 895.
[19] G. J. Augustine, *Curr. Opin. Neurobiol.* **2001**, *11*, 320.
[20] I. I. Kruman, M. P. Mattson, *J. Neurochem.* **1999**, *72*, 529.

